

# Synthesis and Solvatochromic Fluorescence of Biaryl Pyrimidine Nucleosides

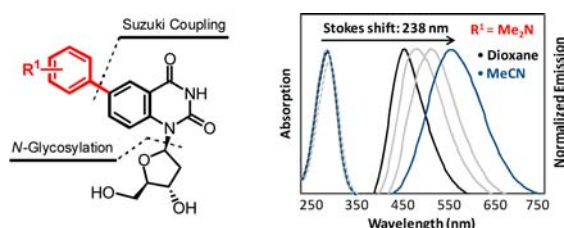
Guillaume Mata and Nathan W. Luedtke\*

Department of Chemistry, University of Zürich, Winterthurerstrasse 190,  
CH-8057 Zürich, Switzerland

luedtke@oci.uzh.ch

Received April 4, 2013

## ABSTRACT



Fluorescent pyrimidine analogs containing a fused biphenyl unit were prepared in high yields using stereoselective *N*-glycosylation and Suzuki–Miyaura cross-coupling reactions. The resulting “push–pull” fluorophores exhibit highly solvatochromic emissions from twisted intramolecular charge-transfer (TICT) states.

Fluorescence spectroscopy is one of the most powerful tools in chemical biology.<sup>1</sup> Fluorescence-based labeling of nucleic acids is widely used for genomic sequencing and for the visualization of DNA replication *in vivo*.<sup>2</sup> The small size and predictable location of fluorescent nucleobase analogs<sup>3</sup> make them ideally suited for monitoring biochemical transformations,<sup>4</sup> conformational changes,<sup>5</sup> and base pairing interactions.<sup>6</sup> The environmental sensitivity

of these probes allows for reporting of microenvironment parameters such as polarity,<sup>7</sup> viscosity,<sup>8</sup> and pH.<sup>9</sup> C-Nucleosides containing arene groups such as pyrene and biphenyl can exhibit high quantum efficiencies of emission (Figure 1A). When incorporated into DNA, they can be used as scaffolds for the construction of multi-chromophore arrays.<sup>10</sup> The incorporation of biphenyl C-nucleosides into duplex DNA has been shown to result in a zipper-like interstrand stacking recognition motif.<sup>11</sup> However, the Watson–Crick hydrogen bonding face in such derivatives is absent, making them poor nucleobase mimics. Given the remarkable photophysical properties of substituted biphenyls,<sup>12</sup> and the need for emissive nucleobase mimics,<sup>3</sup> we designed nucleoside analogs **1a–1h** (Figure 1B). These new analogs contain a biphenyl unit fused to thymidine in a way that should be compatible with

(1) (a) Lakowicz, J. R. *Principles of Fluorescence Spectroscopy*; Springer: New York, 2006. (b) Lavis, L. D.; Raines, R. T. *ACS Chem. Biol.* **2008**, *3*, 142. (c) Sletten, E. M.; Bertozzi, C. R. *Acc. Chem. Res.* **2011**, *44*, 666.

(2) (a) Bao, G.; Rhee, W. J.; Tsourkas, A. *Annu. Rev. Biomed. Eng.* **2009**, *11*, 25. (b) Neef, A. B.; Luedtke, N. W. *Proc. Natl. Acad. Sci. U.S.A.* **2011**, *108*, 20404.

(3) Sinkeldam, R. W.; Greco, N. J.; Tor, Y. *Chem. Rev.* **2010**, *110*, 2579.

(4) (a) Srivatsan, S. G.; Greco, N. J.; Tor, Y. *Angew. Chem., Int. Ed.* **2008**, *47*, 6661. (b) Xie, Y.; Maxson, T.; Tor, Y. *J. Am. Chem. Soc.* **2010**, *132*, 11896.

(5) Luedtke, N. W.; Dumas, A. *J. Am. Chem. Soc.* **2010**, *132*, 18004.

(6) (a) Xie, Y.; Maxson, T.; Tor, Y. *Org. Biomol. Chem.* **2010**, *8*, 5053. (b) Michel, J.; Gueguen, G.; Vercauteren, J.; Moreau, S. *Tetrahedron* **1997**, *53*, 8457. (c) Xie, Y.; Dix, A. V.; Tor, Y. *J. Am. Chem. Soc.* **2009**, *131*, 17605. (d) Greco, N. J.; Tor, Y. *J. Am. Chem. Soc.* **2005**, *127*, 10784.

(7) Sinkeldam, R. W.; Greco, N. J.; Tor, Y. *ChemBioChem* **2008**, *9*, 706.

(8) Sinkeldam, R. W.; Wheat, A. J.; Boyaci, H.; Tor, Y. *Chem-PhysChem* **2011**, *12*, 567.

(9) (a) Sun, K. M.; McLaughlin, C. K.; Lantero, D. R.; Manderville, R. A. *J. Am. Chem. Soc.* **2007**, *129*, 1894. (b) Riedl, J.; Pohl, R.; Rulisek, L.; Hocek, M. *J. Org. Chem.* **2012**, *77*, 1026.

(10) (a) Teo, Y. N.; Kool, E. T. *Chem. Rev.* **2012**, *112*, 4221. (b) Malinovskii, V. L.; Wenger, D.; Haner, R. *Chem. Soc. Rev.* **2010**, *39*, 410.

(11) (a) Brotschi, C.; Leumann, C. J. *Angew. Chem., Int. Ed.* **2003**, *42*, 1655. (b) Zahn, A.; Leumann, C. J. *Chem.—Eur. J.* **2008**, *14*, 1087.

(12) For general reviews about twisted intramolecular charge transfer (TICT) states, see: (a) Bhattacharyya, K.; Chowdhury, M. *Chem. Rev.* **1993**, *93*, 507. (b) Rettig, W. *Angew. Chem., Int. Ed. Engl.* **1986**, *25*, 971. For photophysical properties of substituted biphenyls, see: (c) Maus, M.; Rettig, W.; Jonusauskas, G.; Lapouyade, R.; Rulliere, C. *J. Phys. Chem. A* **1998**, *102*, 7393. (d) Maus, M.; Rettig, W.; Bonafoux, D.; Lapouyade, R. *J. Phys. Chem. A* **1999**, *103*, 3388. (e) Maus, M.; Rettig, W. *Chem. Phys. Lett.* **2000**, *324*, 57.

Previous Work:  
A. Chromophoric Bases



This Work:  
B. Fluorophores **1a–1h**

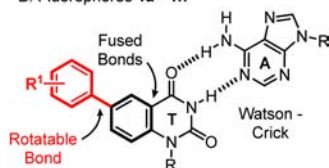


**Figure 1.** (A) Chromophoric *C*-nucleosides containing pyrene and biphenyl. (B) Emissive biaryl nucleoside analogs **1a–1h**. **R** = 2'-deoxyribose, **R**<sup>1</sup> = electron-withdrawing or -donating group.

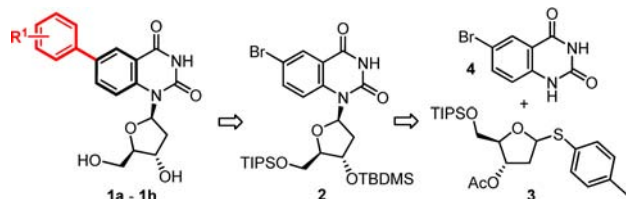
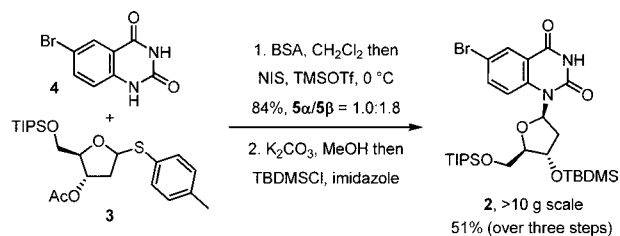


**Figure 2.** Key steps toward the synthesis of **1a–1h**.

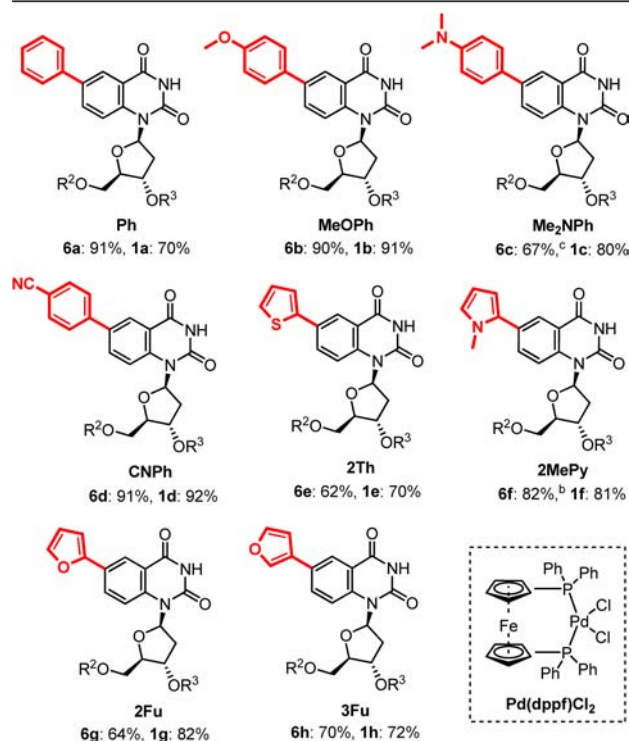
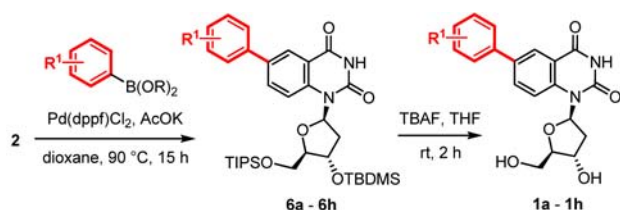
proper Watson–Crick base pairing.<sup>6a–c</sup> Herein, we describe the synthesis and evaluation of these new fluorescent nucleobase analogs and provide a detailed analysis of their structure–photophysical properties relationships.

The synthesis of the biaryl nucleosides **1a–1h** was envisioned from the silylated 6-bromo-quinazoline-2,4-(3*H*)-dione nucleoside **2** via a Pd-catalyzed Suzuki–Miyaura cross-coupling (Figure 2). In this approach, **2** provides a versatile intermediate for the coupling of various boronic acids and esters. Nucleoside **2** can be obtained from a stereoselective *N*-glycosylation of 2-deoxythioriboside **3** with 6-bromo-quinazoline-2,4-(1*H*,3*H*)-dione **4**. According to our new method,<sup>13</sup> 2-deoxythioriboside **3** was *N*-glycosylated with **4** using the combination of *N*,*O*-bis-(trimethylsilyl)-acetamide (BSA), *N*-iodosuccinimide (NIS), and trimethylsilyl trifluoromethanesulfonate (TMSOTf) to afford **5** in 84% yield (**5α/5β** = 1.0:1.8, > 10 g scale, Scheme 1). To facilitate cross-coupling reactions, the C'3-acetate of **5β** was converted into a C'3-silyl ether to give **2** in 95% yield over two steps.<sup>14</sup> Suitable conditions for Pd-catalyzed Suzuki–Miyaura cross-coupling between **2** and phenyl boronic acid were evaluated by screening various palladium sources, ligands, bases, and solvents.<sup>15</sup> Pd(dppf)Cl<sub>2</sub> and AcOK in dioxane at 90 °C were found to be highly effective for this transformation. The biphenyl product **6a** (“Ph”) was

**Scheme 1.** Stereoselective *N*-Glycosylation of 2-Deoxythioriboside **3** and Synthesis of Key Intermediate **2**



**Scheme 2.** Pd-Catalyzed Suzuki–Miyaura Cross-Coupling<sup>a</sup> and Silyl Groups Deprotection



<sup>a</sup> Reagents and conditions: **2** (1.0 equiv), Ar–B(OR)<sub>2</sub> (1.5 equiv), AcOK (1.5 equiv), Pd(dppf)Cl<sub>2</sub> (0.05 equiv), dioxane (0.07 M), 90 °C, 15 h. <sup>b</sup> Ar–B(OR)<sub>2</sub> (2.0 equiv) and AcOK (2.0 equiv) were used. <sup>c</sup> The reaction was performed on a 4.0 g scale. **6a–6h**: R<sup>2</sup> = TIPS, R<sup>3</sup> = TBDMS; **1a–1h**: R<sup>2</sup> = R<sup>3</sup> = H.

isolated in 91% yield (Scheme 2). Electron-donating and -withdrawing groups on the phenyl boronic acid were well tolerated, giving good to excellent yields for biphenyl derivatives **6b–6d** (“MeOPh”, 90%), (“Me<sub>2</sub>NPh”, 67%, performed on a 4.0 g scale), and (“CNPh”, 91%).

(13) Mata, G.; Luedtke, N. W. *J. Org. Chem.* **2012**, *77*, 9006.

(14) The influence of the protecting groups on the sugar moiety in Pd-catalyzed cross-coupling has already been examined. The bulky TBDMS group prevents coordination of the Pd catalyst. For a review about Pd-assisted routes to nucleosides, see: Agrofoglio, L. A.; Gillaizeau, I.; Saito, Y. *Chem. Rev.* **2003**, *103*, 1875.

(15) Test reactions indicated that Pd(dppf)Cl<sub>2</sub> is a superior catalyst as compared to Pd(PPh<sub>3</sub>)<sub>2</sub>Cl<sub>2</sub>, Pd<sub>2</sub>(dba)<sub>3</sub>/SPHOS, and Pd(OAc)<sub>2</sub>/SPHOS. Furthermore, dioxane was found to be superior to toluene and DMF.

**Table 1.** Photophysical Data of Emissive Nucleosides **1a–1h**

| <b>1a–1h</b>             | solvent | $\lambda_{\text{abs}}^a$ | $\lambda_{\text{em}}^b$ | Stokes <sup>c</sup> | $\epsilon^d$ | $\Phi^e$ |
|--------------------------|---------|--------------------------|-------------------------|---------------------|--------------|----------|
| <b>Ph</b>                | dioxane | 270                      | 371                     | 10.1                | 2.49         | 0.11     |
| <b>(1a)</b>              | water   | 269                      | 404                     | 12.4                |              | 0.085    |
| <b>MeOPh</b>             | dioxane | 280                      | 390                     | 10.1                | 2.74         | 0.132    |
| <b>(1b)</b>              | water   | 276                      | 462                     | 14.6                |              | 0.035    |
| <b>Me<sub>2</sub>NPh</b> | dioxane | 312                      | 459                     | 10.3                | 2.01         | 0.071    |
| <b>(1c)</b>              | water   | 297                      | 460                     | 11.9                |              | 0.010    |
| <b>CNPh</b>              | dioxane | 293                      | 362                     | 6.5                 | 2.07         | 0.206    |
| <b>(1d)</b>              | water   | 286                      | 388                     | 7.4                 |              | 0.140    |
| <b>2Th</b>               | dioxane | 298                      | 391                     | 8.0                 | 2.02         | 0.094    |
| <b>(1e)</b>              | water   | 295                      | 449                     | 11.6                |              | 0.024    |
| <b>2MePy</b>             | dioxane | 292                      | 432                     | 11.1                | 1.92         | 0.079    |
| <b>(1f)</b>              | water   | 286                      | 375                     | 8.3                 |              | 0.001    |
| <b>2Fu</b>               | dioxane | 292                      | 403                     | 9.4                 | 3.03         | 0.152    |
| <b>(1g)</b>              | water   | 290                      | 463                     | 12.9                |              | 0.038    |
| <b>3Fu</b>               | dioxane | 269                      | 381                     | 10.9                | 1.87         | 0.086    |
| <b>(1h)</b>              | water   | 267                      | 430                     | 14.2                |              | 0.075    |

<sup>a</sup>  $\lambda_{\text{abs}}$  are reported at the maximum absorbance wavelength in nm. <sup>b</sup>  $\lambda_{\text{em}}$  in nm. <sup>c</sup> Stokes shifts are reported in  $10^3 \text{ cm}^{-1}$ . <sup>d</sup> Extinction coefficients ( $\epsilon$ ) are given at  $\lambda_{\text{max}}$  in  $\text{H}_2\text{O}$  and are reported in  $10^4 \text{ M}^{-1} \text{ cm}^{-1}$ . <sup>e</sup> 2-Aminopyridine in 0.1 N  $\text{H}_2\text{SO}_4$  ( $\Phi = 0.60$ ) was used as the fluorescent standard for the relative quantum yields ( $\Phi$ ) of **1a–1h**. (See SI for complete fluorescence data, spectra and plots.)

**Figure 3.** Molecular orbital plot of the isolated nucleobase of **1a** (see SI for DFT calculation details).

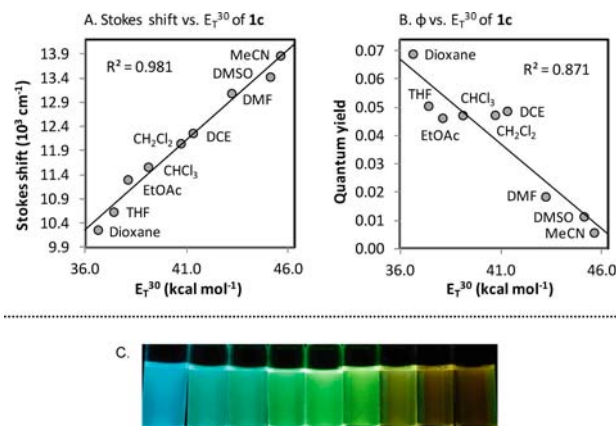
This approach is also compatible with the synthesis of derivatives containing five-membered heteroaromatic groups **6e–6h**. It is known that five-membered, 2-heteroaromatic boronic acids are prone to undergo protodeboronation under basic conditions,<sup>16</sup> but reactions involving **2** and thiophene, pyrrole, or furan boronic acids furnished the corresponding biaryls **6e–6h** in good isolated yields (“**2Th**”, 62%), (“**2MePy**”, 82%), (“**2Fu**”, 64%), and (“**3Fu**”, 70%). Treating nucleosides **6a–6h** with TBAF in THF afforded the deprotected compounds **1a–1h** in isolated yields ranging from 70% to 92% (Scheme 2), and in high purity (> 98%) according to  $^1\text{H}$  NMR.<sup>17</sup>

The photophysical properties of **1a–1h** are summarized in Table 1. The quantum yields of these compounds are moderate in water ( $\Phi = 0.14–0.0002$ ) and in dioxane ( $\Phi = 0.21–0.07$ ). These values are very similar to biphenyl

(16) (a) Kinzel, T.; Zhang, Y.; Buchwald, S. L. *J. Am. Chem. Soc.* **2010**, *132*, 14073. (b) Thakur, A.; Zhang, K.; Louie, J. *Chem. Commun.* **2012**, 48, 203.

(17) In addition to column chromatography, extensive washing of the products with MeOH and  $\text{H}_2\text{O}/\text{AcOH}$  was used to eliminate traces of TBAF salts. See SI for  $^1\text{H}$  and  $^{13}\text{C}$  NMR spectra.

(18) Berlman, I. B. *Handbook of Fluorescence Spectra of Aromatic Molecules*; Academic Press: 1971.

**Figure 4.** (A) Plot between the Stokes shift of **1c** and  $E_T^{30}$  value. (B) Plot between the quantum yield of **1c** and  $E_T^{30}$  value. (C) Photograph of **1c** (fixed concentration) in organic solvents of increasing polarity with UV–B irradiation.

itself ( $\Phi = 0.18$ ),<sup>18</sup> but the wavelengths of excitation and emission of **1a–1h** are red-shifted. For example, the maximal wavelengths of absorbance and emission of the biphenyl nucleoside **Ph** ( $\lambda_{\text{abs}} = 270 \text{ nm}$ ,  $\lambda_{\text{em}} = 371 \text{ nm}$ ) are 23 and 59 nm to the red of biphenyl in dioxane ( $\lambda_{\text{abs}} = 247 \text{ nm}$ ,  $\lambda_{\text{em}} = 312 \text{ nm}$ ). The reason for this red-shifted emission is related to the ability of the pyrimidine group to serve as an electron-accepting group upon photoexcitation. DFT calculations indicate charge transfer from the benzene group of **Ph** to pyrimidine upon going from HOMO  $\rightarrow$  LUMO (Figure 3). These results suggest the presence of a push–pull system where the pyrimidine group acts as an electron acceptor in the excited state. The magnitude of this push–pull effect is augmented by electron-donating groups in **1b** and **1c**, but diminished by the cyano group in **1d**. Indeed, the calculated HOMO–LUMO gaps ( $\text{Me}_2\text{NPh} < \text{MeOPh} < \text{Ph} < \text{CNPh}$ , see Supporting Information (SI)) were inversely correlated with the Stokes shifts of these compounds in dioxane (Table 1). Taken together, these results are consistent with the presence of emissive TICT states that are stabilized by electron-donating groups on the benzene ring.<sup>12</sup>

To characterize the environmental sensitivity of **1a–1h**, the maximal wavelengths for absorbance and emission were measured in different solvents, and the Stokes shifts were plotted against Reichardt’s solvent polarity parameter ( $E_T^{30}$ ).<sup>19</sup> Consistent with the presence of a twisted biaryl bond in the ground state of these molecules (see SI for DFT calculations), the absorption maxima of **1a–1h** were relatively insensitive to solvent polarity. The Stokes shifts of these compounds are highly solvatochromic due to changes in their emission wavelengths. For example, the Stokes shift of **Me<sub>2</sub>NPh** increased from  $10.3 \times 10^3 \text{ cm}^{-1}$  in dioxane ( $\lambda_{\text{em}} = 459 \text{ nm}$ ) to  $13.9 \times 10^3 \text{ cm}^{-1}$  in MeCN ( $\lambda_{\text{em}} = 550 \text{ nm}$ ) to give an exceptionally large slope of  $373 \text{ cm}^{-1}/\text{kcal mol}^{-1}$  (Figure 4A).

(19) (a) Reichardt, C. *Chem. Rev.* **1994**, *94*, 2319. (b) Sinkeldam, R. W.; Tor, Y. *Org. Biomol. Chem.* **2007**, *5*, 2523.

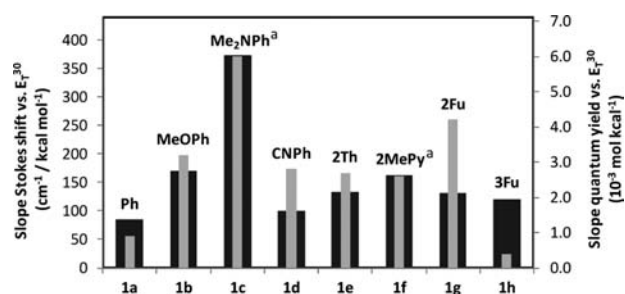


**Figure 5.** Sensitivity of the nucleosides **1a–1h** toward solvent polarity in dioxane, water, and their mixtures. The black bars represent the slope of the Stokes shift and  $E_T^{30}$  value. The gray bars represent the slope of the fluorescence quantum yield and  $E_T^{30}$  value. <sup>a</sup> Due to quenching by  $H_2O$ , slopes were determined in organic solvents for **1c** and **1f**.

This effect can easily be observed under UV illumination, where samples of **Me<sub>2</sub>NPh** appear bright blue to dark orange, depending on the solvent polarity (Figure 4C).

The emission intensity of **Me<sub>2</sub>NPh** is highly sensitive to solvent polarity, with a slope of  $0.006 \text{ mol kcal}^{-1}$  from  $\Phi = 0.071$  in dioxane to  $\Phi = 0.008$  in MeCN (Figure 4B). **Me<sub>2</sub>NPh** exhibits a low quantum yield in water ( $\Phi = 0.010$ ) that is 2.7-fold higher in  $D_2O$  ( $\Phi = 0.027$ , Table S3A SI). This type of kinetic isotope effect suggests the presence of proton-transfer reactions between the excited fluorophore and bulk solvent that can facilitate nonemissive decay in water.

Consistent with the presence of emissive TICT states,<sup>12</sup> the emissions from **1a–1h** exhibit red-shifting and lower quantum yields with increasing solvent polarity. The magnitudes of these effects are compared in Figure 5. The biphenyl derivatives containing electron-donating substituents **MeOPh** and **Me<sub>2</sub>NPh** exhibit highly solvatochromic Stokes shifts and quantum yields. In contrast, **CNPh** exhibits diminished solvent sensitivity, and a good quantum yield over the entire range of solvent polarity tested ( $\Phi = 0.206–0.140$ ). Together these results are consistent with "push–pull" TICT fluorophores.<sup>12</sup> The trends between the compounds containing a five-membered heterocyclic ring **1e–1h** are somewhat more complicated. For example, **2Fu** exhibits quantum yields that are highly sensitive to solvent polarity ( $4.2 \times 10^{-3} \text{ mol kcal}^{-1}$ ), whereas its isomer, **3Fu**, exhibits very little sensitivity ( $0.3 \times 10^{-3} \text{ mol kcal}^{-1}$ ).

To systematically compare the theoretical and experimental photophysical properties of the biphenyl derivatives **1a–1d** with the biaryl derivatives **1e–1h**, the calculated HOMO–LUMO gap for each compound was plotted against its peak emission wavelength in dioxane to give an excellent linear correlation ( $R^2 = 0.981$ ,

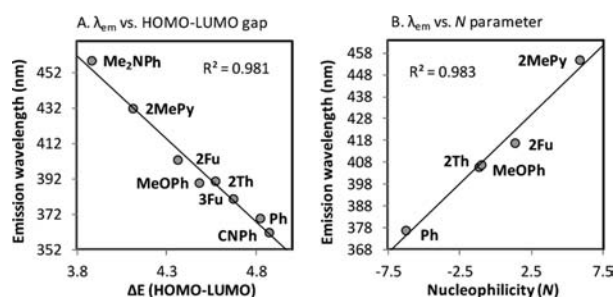


**Figure 6.** (A) Plot between the emission wavelength of **1a–1h** and calculated HOMO–LUMO energy gaps (see SI for calculation details). (B) Plot between the emission wavelength of the nucleosides **1a–1h** and Mayr's nucleophilicity parameter ( $N$ ) of the isolated aryl groups ( $R^1$ ) for benzene, anisole, thiophene,  $N$ -methylpyrrole, and furan in  $CH_2Cl_2$ .<sup>20</sup>

Figure 6A). These results suggested that the underlying photophysical processes are similar for **1a–1h**, where electron-donating groups cause smaller HOMO–LUMO gaps and red-shifted emissions as compared to electron-withdrawing groups. This conclusion is further supported by plotting the emission wavelength of each nucleoside versus the Mayr's nucleophilicity parameter ( $N$ ) for the isolated aryl/heteroaryl group " $R^1$ ".<sup>20</sup> An excellent linear correlation between these factors is observed ( $R^2 = 0.983$ , Figure 6B). This unusual approach reveals a possible method to extrapolate nucleophilicity parameters of groups that cannot be experimentally measured. For example, this plot can be used to predict a nucleophilicity parameter for the position 3 of furan ( $N \approx -4.12$ ) based upon the emission wavelength of **3Fu** ( $\lambda_{em} = 388 \text{ nm}$ ) in  $CH_2Cl_2$ .

In summary, we have synthesized a new family of fluorescent biaryl pyrimidines in high yield and purity. The nucleosides exhibit highly solvatochromic emissions from twisted intramolecular charge-transfer (TICT) states. Previous studies have demonstrated fluorescent emissions resulting from charge-transfer recombination in pyrene-modified deoxyuridine,<sup>21</sup> but to the best of our knowledge, compounds **1a–h** provide the first examples of nucleobase analogs that are "classical" TICT fluorophores.<sup>12</sup> **Me<sub>2</sub>NPh** (**1c**) exhibits absorbance well to the red of unmodified DNA nucleobases and emissions that are exceptionally sensitive to solvent polarity. **Me<sub>2</sub>NPh** is therefore a promising candidate for investigating local DNA conformational changes by reporting changes in microenvironmental polarity and solvation.<sup>5</sup>

**Acknowledgment.** This work was supported by the Swiss National Science Foundation (#130074) and the University of Zürich.

**Supporting Information Available.** Figures S1–12, Tables S1–S8, experimental procedures, spectroscopic characterizations, fluorescence spectra, molecular orbital plots, and  $^1H$  and  $^{13}C$  NMR spectra. This material is available free of charge via the Internet at <http://pubs.acs.org>.

The authors declare no competing financial interest.

(20) (a) Gotta, M. F.; Mayr, H. *J. Org. Chem.* **1998**, *63*, 9769. (b) Mayr, H.; Bug, T.; Gotta, M. F.; Hering, N.; Irrgang, B.; Janker, B.; Kempf, B.; Loos, R.; Ofial, A. R.; Remennikov, G.; Schimmel, H. *J. Am. Chem. Soc.* **2001**, *123*, 9500. (c) Ammer, J.; Nolte, C.; Mayr, H. *J. Am. Chem. Soc.* **2012**, *134*, 13902. (d) Mayr, H.; Ofial, A. R. *J. Phys. Org. Chem.* **2008**, *21*, 584. (e) Mayr, H.; Kempf, B.; Ofial, A. R. *Acc. Chem. Res.* **2003**, *36*, 66.

(21) Netzel, T. L.; Zhao, M.; Nafisi, K.; Headrick, J.; Sigman, M. S.; Eaton, B. E. *J. Am. Chem. Soc.* **1995**, *117*, 9119.